

Spin Dynamics and Orbital State in LaTiO₃

B. Keimer^{1,2}, D. Casa², A. Ivanov³, J.W. Lynn⁴, M. v. Zimmermann⁵,
J.P. Hill⁵, D. Gibbs⁵, Y. Taguchi⁶, and Y. Tokura⁶

¹ *Max-Planck-Institut für Festkörperforschung, 70569 Stuttgart, Germany*

² *Department of Physics, Princeton University, Princeton, NJ 08544*

³ *Institut Laue-Langevin, 156X, 38042 Grenoble Cedex 9, France*

⁴ *NIST Center for Neutron Research, National Institute of Standards and Technology, Gaithersburg, MD 20899*

⁵ *Department of Physics, Brookhaven National Laboratory, Upton, NY 11973*

⁶ *Department of Applied Physics, University of Tokyo, Tokyo 113, Japan*

(November 18, 2018)

A neutron scattering study of the Mott-Hubbard insulator LaTiO₃ ($T_N = 132$ K) reveals a spin wave spectrum that is well described by a nearest-neighbor superexchange constant $J = 15.5$ meV and a small Dzyaloshinskii-Moriya interaction ($D = 1.1$ meV). The nearly isotropic spin wave spectrum is surprising in view of the absence of a static Jahn-Teller distortion that could quench the orbital angular momentum, and it may indicate strong orbital fluctuations. A resonant x-ray scattering study has uncovered no evidence of orbital order in LaTiO₃.

In the layered cuprates exemplified by the series La_{2-x}Sr_xCuO_{4+δ}, the transition from a $3d^9$ antiferromagnetic (AF) insulator at $x = \delta = 0$ into an unconventional metallic and superconducting state with increasing hole concentration ($x, \delta > 0$) has received an enormous amount of attention. The magnetic spectra of these materials, revealed by inelastic neutron scattering, have played a key role in efforts to arrive at a theoretical explanation of this transition. The pseudocubic perovskite La_{1-x}Sr_xTiO_{3+δ} undergoes an analogous transition from a $3d^1$ AF insulator at $x = \delta = 0$ to a metallic state with increasing hole concentration [1]. In the titanates, however, the metallic state shows conventional Fermi liquid behavior, and no superconductivity is found [1]. Momentum-resolved probes such as angle-resolved photoemission spectroscopy and inelastic neutron scattering have thus far not been applied to the titanates, and the origin of the very different behavior of the metallic cuprates and titanates is still largely unexplored. Here we report an inelastic neutron scattering and anomalous x-ray scattering study of the parent compound of the titanate series, LaTiO₃, that provides insight into the microscopic interactions underlying this behavior.

Orbital degrees of freedom, quenched in the layered cuprates by a large Jahn-Teller (JT) distortion of the CuO₆ octahedra, are likely to be a key factor in the phenomenology of the titanates. While the TiO₆ octahedra are *tilted* in a GdFeO₃-type structure, their *distortion* is small and essentially undetectable in neutron powder diffraction experiments on LaTiO₃ (Ref. [2]). The crystal field acting on the Ti³⁺ ion is therefore nearly cubic, and heuristically one expects a quadruply degenerate single-ion ground state with unquenched orbital angular momentum opposite to the spin angular momentum due to the spin-orbit interaction. In other perovskites such as LaMnO₃, such spin-orbital degeneracies are broken by successive orbital and magnetic ordering transitions

[3]. In the orbitally and magnetically ordered state of LaMnO₃, the spin wave spectrum is highly anisotropic reflecting the different relative orientations of the orbitals on nearest-neighbor Mn atoms in different crystallographic directions [4].

The reduced ordered moment ($\mu_0 \sim 0.45\mu_B$, Ref. [5]) in the G-Type AF structure of LaTiO₃ (inset in Fig. 1) at first sight appears consistent with a conventional scenario in which the orbital occupancies at every site are established at some high temperature, and the magnetic degrees of freedom (coupled spin and orbital angular momenta) order at a lower temperature. Full theoretical calculations, however, generally predict a ferromagnetic spin structure for LaTiO₃ [6]. As in LaMnO₃, the spin dynamics of LaTiO₃ are highly sensitive to the orbital occupancies and can provide important information in this regard. We find that the exchange anisotropy is small and hence inconsistent with the presence of an appreciable unquenched orbital moment. At the same time, synchrotron x-ray scattering experiments have not revealed any evidence of reflections showing a resonant enhancement at the Ti K-edge, unlike other perovskites in which orbital order (OO) is present. These observations, along with previously puzzling Raman scattering data [7], indicate strong fluctuations in the orbital sector of LaTiO₃.

The neutron scattering experiments were conducted on the BT2 and BT4 triple axis spectrometers at the NIST research reactor and at the IN8 spectrometer at the Institut Laue-Langevin. For excitation energies up to 25 meV, we used high resolution configurations with vertically focusing pyrolytic graphite (PG) (002) monochromator and PG (002) analyser crystals set for final neutron energies of 14.7 meV or 30.5 meV and horizontally collimated beams at both NIST and ILL. For excitation energies of 20 meV and higher, we used a double-focusing analyser on IN8 with open collimations, and with a Cu (111) monochromator and a PG (002) analyser set for

a final neutron energy of 35 meV. PG filters were used in the scattered beam to reduce higher order contamination. Data obtained on the different spectrometers and with different configurations were in good agreement.

The sample was a single crystal of volume 0.2 cm^3 and mosaicity 0.5° grown by the floating zone technique. It is semiconducting, and neutron diffraction (Fig. 1) shows a sharp, second-order Néel transition at $T_N = 132 \text{ K}$, implying a highly homogeneous oxygen content ($\delta \sim 0.01$ in $\text{LaTiO}_{3+\delta}$) [1]. The diffraction pattern is consistent with the G-type structure found previously [5], and a small uncompensated moment ($\sim 10^{-2} \mu_B$ per Ti spin at low temperatures) appears below T_N due to spin canting, as observed by magnetization measurements. The nuclear structure of LaTiO_3 is orthorhombic (space group Pnma [2]), but the crystal is fully twinned. Because of the isotropy of the spin wave dispersions (see below), twinning did not influence the neutron measurements. For simplicity we express the wave vectors in the pseudocubic notation with lattice constant $a \sim 3.95 \text{ \AA}$. In this notation, AF Bragg reflections are located at $(h/2, k/2, l/2)$ with h, k, l odd. Data were taken with the crystal in two different orientations in which wave vectors of the form (h, h, l) or $(h, k, (h+k)/2)$, respectively, were accessible.

Fig. 2 shows inelastic neutron scattering data obtained in constant- \mathbf{q} mode with high resolution near the AF zone center. The dispersing peak shown disappears above the Néel temperature, thus clearly identifying itself as a spin wave excitation. In Fig. 3, constant-energy scans obtained in the high-intensity configuration with relaxed resolution are presented. The profile shapes are strongly influenced by the spectrometer resolution, and a deconvolution is required to accurately extract the positions of the spin wave peaks. For the high-resolution configuration with only vertical focusing we used the standard Cooper-Nathans procedure while a Monte-Carlo ray-tracing routine was used for the doubly focused geometry [8]. An analytical approximation to the Ti^{3+} form factor and the standard intensity factors for AF magnons were incorporated in the programs [9]. The peak positions thus obtained are shown in Fig. 4 in the (111) direction.

A very good global fit to all data was obtained by convoluting the resolution function with a single spin wave branch of the generic form $\hbar\omega = zSJ\sqrt{(1+\epsilon)^2 - \gamma^2}$ where $\hbar\omega$ is the spin wave energy, $z = 6$ is the coordination number, $S = 1/2$ is the Ti spin, $J = 15.5 \pm 1 \text{ meV}$ is the isotropic (Heisenberg) part of the nearest-neighbor superexchange [10], $\gamma = \frac{1}{3}[\cos(q_x a) + \cos(q_y a) + \cos(q_z a)]$ with the magnon wave vector \mathbf{q} measured from the magnetic zone center, and the zone center gap is $\Delta \sim zSJ\sqrt{2\epsilon} = 3.3 \pm 0.3 \text{ meV}$. The solid lines in Figs. 2-4 result from this global fit and obviously provide a good description of all data. Inclusion of further-neighbor interactions, damping parameters above the instrumental resolution, or other (nonde-

generate) spin wave branches did not improve the fit.

The Heisenberg exchange constant J is in fair agreement with predictions based on a comparison of the Néel temperature with numerical simulations ($T_N = 0.946J/k_B \sim 170 \text{ K}$ for spins-1/2 on a simple cubic lattice [11]). In general, the spin wave gap is determined by symmetric and antisymmetric (Dzyaloshinskii-Moriya) anisotropy terms in the superexchange matrix, by terms originating from direct exchange, by dipolar interactions, and by the single ion anisotropy. The latter two effects are negligible and nonexistent, respectively, in spin-1/2 systems. In the GdFeO_3 structure, antisymmetric exchange is allowed by symmetry, and its magnitude is expected to scale with the tilt angle of the TiO_6 octahedra. Because of the large tilt angle (11.5°), we expect this effect to dominate over the more subtle direct exchange terms. Theories of superexchange anisotropies [12] were recently reexamined [13] in the light of neutron scattering data on the layered cuprates. It was shown that the symmetric and antisymmetric terms are related by a hidden symmetry so that the two zone-center spin wave gaps depend on the relationship between Dzyaloshinskii-Moriya (DM) vectors centered on each magnetic bond. Specifically, for two-dimensional (2D) spin structures (such as the one of La_2CuO_4) the gaps are degenerate if all DM vectors have the same magnitude, and the degenerate gaps are nonzero if, in addition, not all vectors have the same orientation. The bond-dependent DM vectors for LaMnO_3 (isostructural to LaTiO_3) were given in Ref. [14]. Although a detailed analysis of the spin dynamics for these 3D systems has not been reported, we note that both of the above criteria are fulfilled for LaTiO_3 . In particular, the DM vectors centered on the six Ti-O-Ti bonds have different orientations but are expected to have the same magnitude because of the practically equal bond lengths and bond angles [2]. Our observation of degenerate but nonzero spin wave gaps therefore provides support for the predictions of Ref. [13] in a 3D, non-cuprate system.

Carrying the analogy to the 2D cuprates one step further, we expect that the anisotropy gap is $\Delta \sim zSD$, and hence $D \sim 1.1 \text{ meV}$ is the net DM interaction per Ti spin. Due to spin canting, the net ferromagnetic moment per spin should therefore be $\sim \mu_0 D/2J = 1.5 \times 10^{-2} \mu_B$, in good agreement with the observed value. This supports our assumption that the DM interaction provides the dominant contribution to the spin wave gap. A microscopic calculation of D would be a further interesting test of the formalism developed in Ref. [13].

The small easy-axis anisotropy in the exchange Hamiltonian of LaTiO_3 is difficult to understand based on simple crystal-field considerations for the Ti^{3+} ion. The antisymmetric exchange is generally of order $(\Delta g/g)J$ where g is the free-electron Landé factor and Δg is its shift in the crystalline environment [12]. Based on our data, we therefore estimate $\Delta g/g \sim 0.05$. On the other hand, in

the absence of any appreciable static JT distortion as observed experimentally [2], one expects that the spin-orbit interaction ($\Lambda \sim +20$ meV [15]) splits the t_{2g} multiplet of the cubic crystal field Hamiltonian into a quadruply degenerate ground state and a higher-lying Kramers doublet. In a simple crystal field model, this ground state is characterized by an unquenched orbital moment equal and antiparallel to the spin moment ($\Delta g/g = 1$). More elaborate Hartree-Fock calculations [6] do not change this picture qualitatively: Even if a static JT distortion at the limits of the experimental error bars [2] is included, the orbital contribution to the moment remains comparable to the spin moment ($\Delta g/g \sim 0.5$). There is thus an order-of-magnitude discrepancy between the predictions of conventional models and the neutron scattering observations. The smallness of the spin anisotropy in LaTiO_3 is underscored by a different comparison: The D/J ratio of LaTiO_3 differs only by a factor of 3 from that of La_2CuO_4 , whose low-temperature ordered moment is in near-perfect agreement with the spin-only prediction. Since D/J scales with the tilt angle of the octahedra which is a factor of ~ 3 larger in LaTiO_3 , the relative magnitude of this quantity in the two materials can be accounted for without invoking a large orbital moment in LaTiO_3 .

Interestingly, the large discrepancy between the predictions of conventional models and the neutron scattering observations has a close analogy in the electron spin resonance (ESR) literature. The description of ESR data on Ti^{3+} impurities embedded into perovskite lattices in fact commonly requires g -factors that are much more isotropic than predicted by simple crystal field calculations [15]. According to a widely used model [16], this is attributed to the dynamical JT effect where the orbital degeneracy is lifted by coupling to zero-point lattice vibrations.

While the dynamical JT effect is well established in impurity systems, it has thus far not been reported in lattice systems which commonly exhibit static, cooperative JT distortions associated with OO. Anomalous x-ray diffraction with photon energies near an absorption edge of the transition metal ion has recently been established as a direct probe of OO in perovskites [3] whose sensitivity far exceeds conventional diffraction techniques that probe OO indirectly through associated lattice distortions. We have therefore carried out an extensive search for reflections characteristic of orbital ordering near the Ti K-edge (4.966 keV) at beamline X22C at the National Synchrotron Light Source, with energy resolution ~ 5 eV. The experiments were performed at low temperature ($T=10\text{K}$) on a polished (1,1,0) surface of the same crystal that was also used for the neutron measurements. No evidence for resonant reflections at several high symmetry positions (such as $(\frac{1}{2}, \frac{1}{2}, 0)$, the ordering wave vector expected for t_{2g} orbitals with a G-type spin structure [17]) was found under the same conditions that enabled their

positive identification in LaMnO_3 [3], YTiO_3 [18] and related materials. If OO is present in LaTiO_3 , we can hence conclude that its order parameter is much smaller than in comparable perovskites. On general grounds, the reduction of the order parameter should be accompanied by enhanced orbital zero-point fluctuations. These may have already been detected (though not identified as such): A large electronic background and pronounced Fano-type phonon anomalies were observed by Raman scattering in nominally stoichiometric, *insulating* titanates and are most pronounced in LaTiO_3 [7]. In the light of our observations, it is of course important to revisit these experiments and rule out any possible role of residual oxygen defects, inhomogeneity, etc. The presently available data are, however, naturally interpreted as arising from orbital fluctuations coupled to lattice vibrations.

An observation not explained by these qualitative considerations is the small ordered moment in the AF state. If the orbital moment is indeed largely quenched, one would naively expect a spin-only moment of $0.85\mu_B$ [19], in contrast to the experimental observation of $0.45\mu_B$. A recently proposed full theory of the interplay between the orbital and spin dynamics in LaTiO_3 has yielded a prediction of the ordered moment that is in quantitative agreement with experiment [20].

In conclusion, several lines of evidence from neutron, x-ray and Raman scattering can be self-consistently interpreted in terms of an unusual many body state with AF long range order but strong orbital fluctuations. This should be an interesting subject of theoretical research. The orbital fluctuations are expected to be enhanced in the presence of itinerant charge carriers and therefore to strongly influence the character of the insulator-metal transition. The present study provides a starting point for further investigations in doped titanates.

We thank A. Aharony, M. Cardona, P. Horsch, D. Khomskii, E. Müller-Hartmann, A. Oles, G. Sawatzky, and especially G. Khaliullin for discussions, and J. Kulda for gracious assistance with his resolution program. The work was supported by the US-NSF under grant No. DMR-9701991, by the US-DOE under contract No. DE-AC02-98CH10886, and by NEDO and Grants-In-Aid from the Ministry of Education, Japan.

-
- [1] Y. Taguchi *et al.*, Phys. Rev. B **59**, 7917 (1999); Y. Tokura *et al.*, Phys. Rev. Lett. **70**, 2126 (1993).
 - [2] D.A. MacLean, H.N. Ng, and J.E. Greedan, J. Solid State Chem. **30**, 35 (1979); M. Eitel and J.E. Greedan, J. Less Common Met. **116**, 95 (1986).
 - [3] Y. Murakami *et al.*, Phys. Rev. Lett. **81**, 582 (1998).
 - [4] F. Moussa *et al.*, Phys. Rev. B **54**, 15149 (1996).

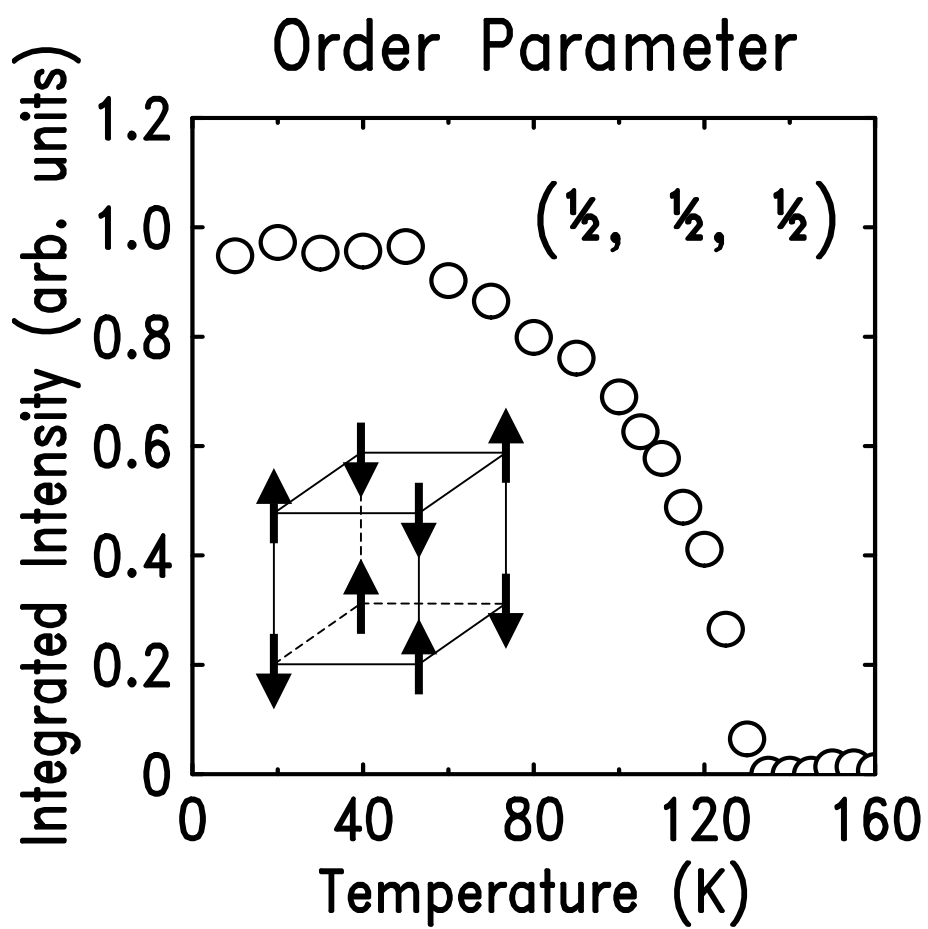
- [5] J.P. Goral and J.E. Greedan, *J. Mag. Mag. Mat.* **37**, 315 (1983).
- [6] T. Mizokawa and A. Fujimori, *Phys. Rev. B* **54**, 5368 (1996); T. Mizokawa, D.I. Khomskii, and G. Sawatzky, *ibid.* **60**, 7309 (1999).
- [7] M. Reedyk *et al.*, *Phys. Rev. B* **55**, 1442 (1997).
- [8] J. Kulda, private communication.
- [9] P.J. Brown in *International Tables for Crystallography*, edited by A.J.C. Wilson (Reidel, Dordrecht, 1995), Vol. C, pp. 391-99.
- [10] J is the superexchange energy per nearest-neighbor pair. In this notation $J \sim 100$ meV in La_2CuO_4 .
- [11] A.W. Sandvik, *Phys. Rev. Lett.* **80**, 5196 (1999).
- [12] T. Moriya, *Phys. Rev.* **120**, 91 (1960).
- [13] T. Yildirim *et al.*, *Phys. Rev. B* **52**, 10239 (1995).
- [14] I. Solovyev, N. Hamada, and K. Terakura, *Phys. Rev. Lett.* **76**, 4825 (1996).
- [15] A. Abragam and B. Bleaney, *Electron Paramagnetic Resonance of Transition Ions* (Oxford University Press, New York, 1970).
- [16] F.S. Ham, *Phys. Rev.* **138**, A1727 (1965); R.M. Macfarlane, J.Y. Wong, and M.D. Sturge, *ibid.* **166**, 250 (1968).
- [17] See, *e.g.*, Y. Ren *et al.*, *Nature* **396**, 441 (1998).
- [18] H. Nakao *et al.*, to be published.
- [19] P.W. Anderson, *Phys. Rev.* **86**, 694 (1952).
- [20] G. Khaliullin and S. Maekawa, *Phys. Rev. Lett.* **85**, 3950 (2000).

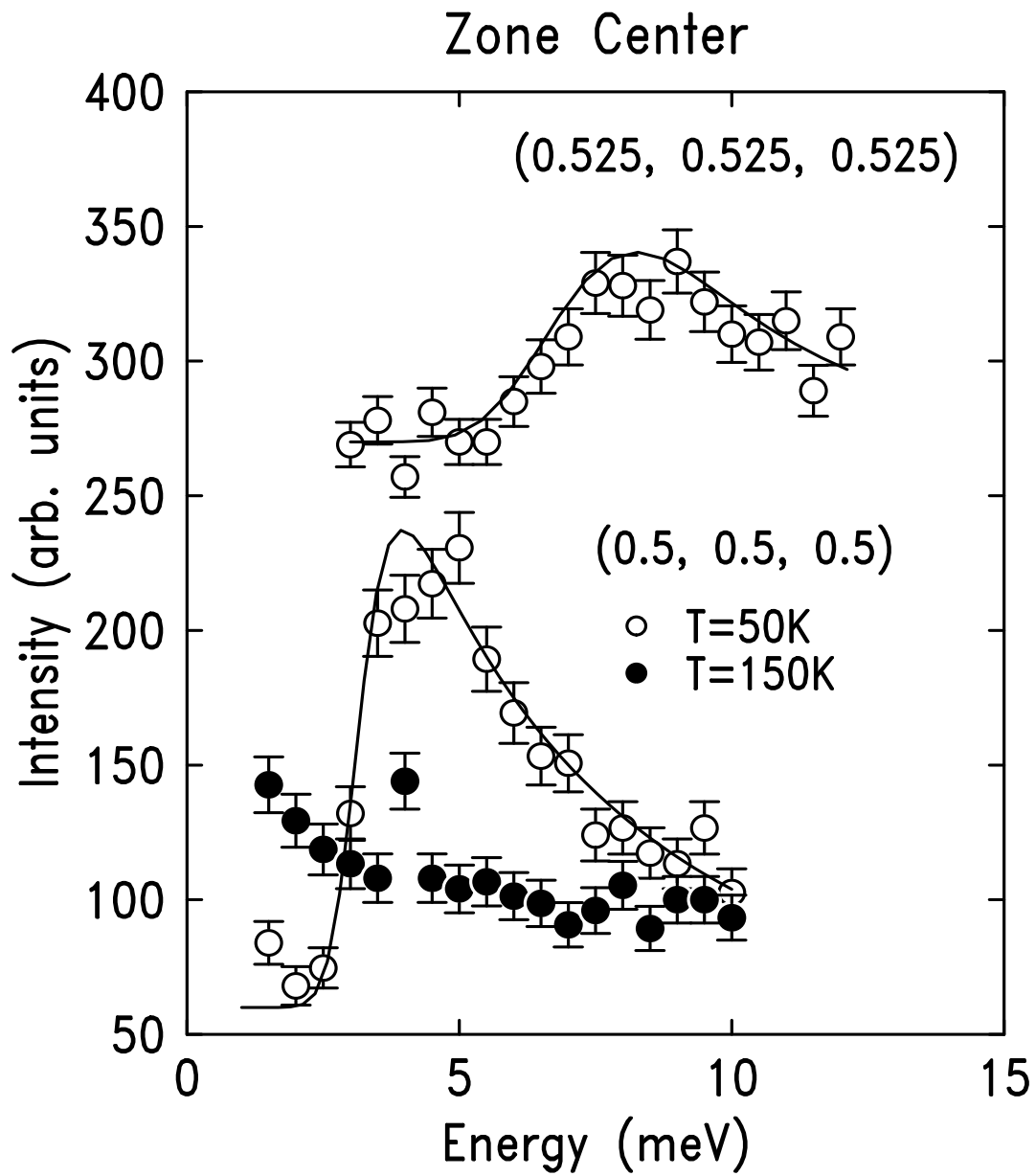
FIG. 1. Integrated intensity of the (0.5,0.5,0.5) AF Bragg reflection as a function of temperature. The inset shows the G-type spin structure.

FIG. 2. Typical constant- \mathbf{q} scans near the AF zone center. The upper profile is offset by 200 units. The lines are the result of a convolution of a spin wave cross section with the instrumental resolution function, as described in the text.

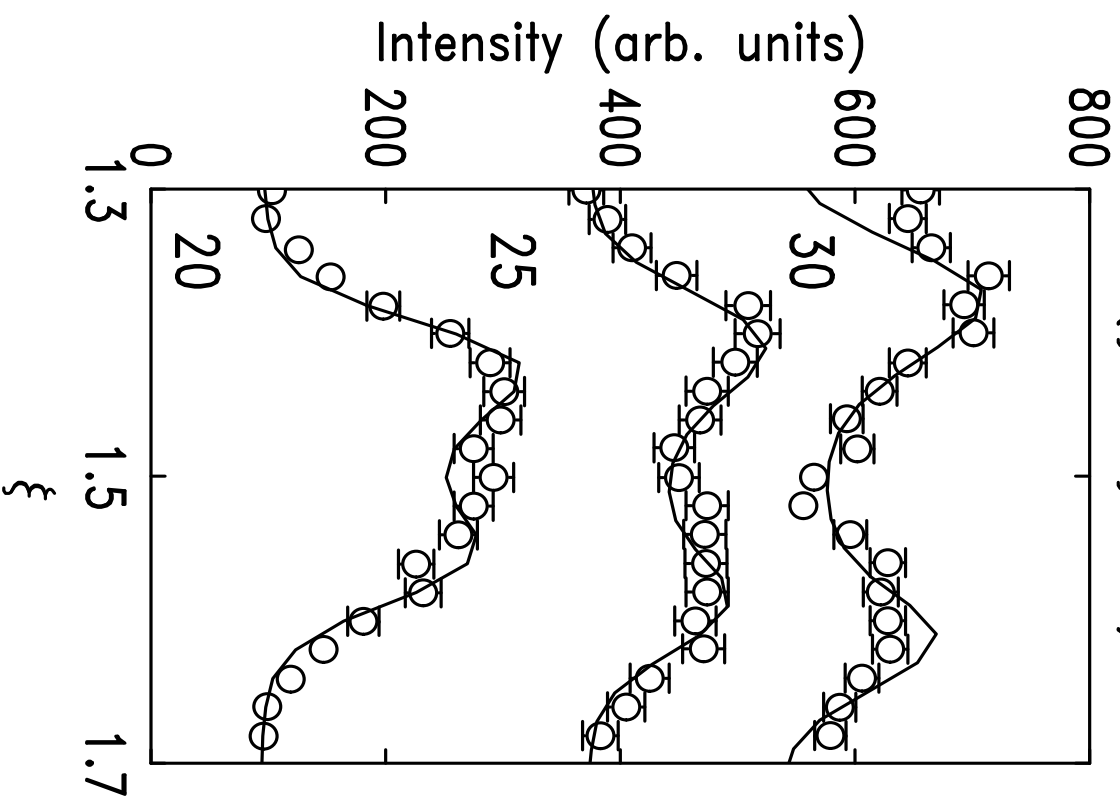
FIG. 3. Typical constant-energy scans in two different directions of reciprocal space. The profiles are labeled by the excitation energy in meV. The lines are the result of a convolution of a spin wave cross section with the instrumental resolution function, as described in the text.

FIG. 4. Fitted spin wave peak positions in the (1,1,1) direction of reciprocal space. The line is the magnon dispersion curve described in the text.

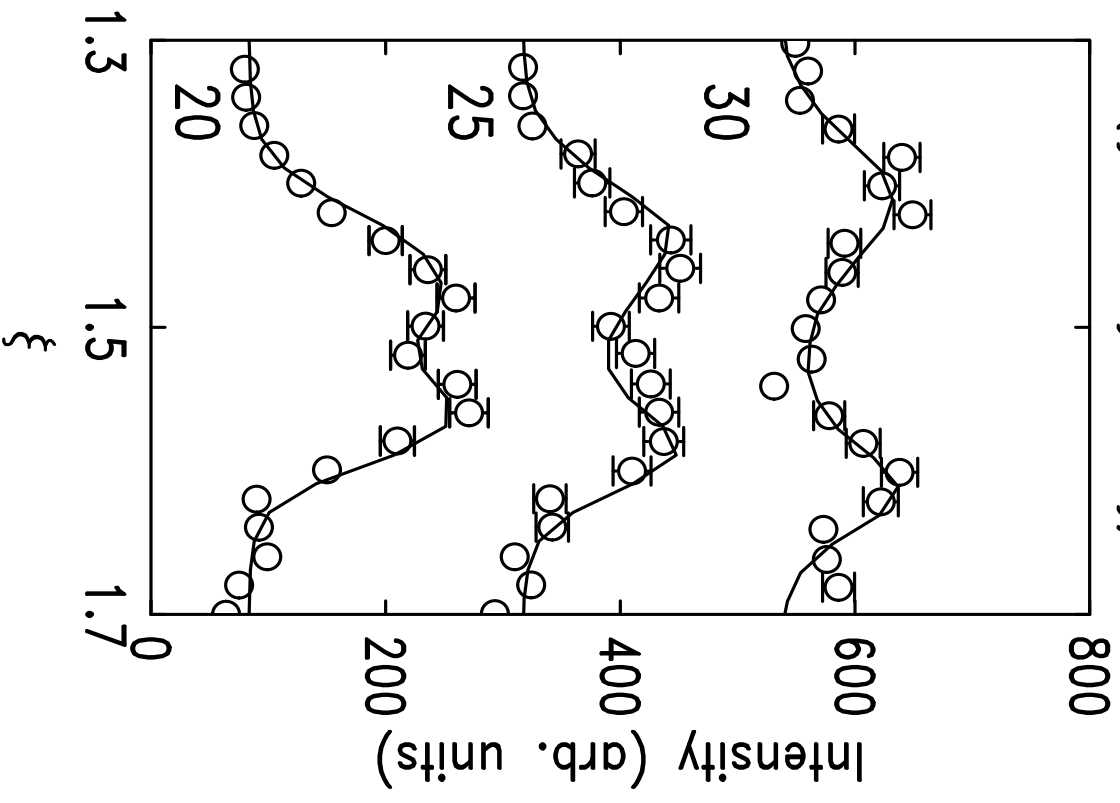




$(\xi, 1-\xi, 0.5)$



$(\xi, -2+\xi, -1+\xi)$



(ξ, ξ, ξ) Spin Waves

